Experimental Investigation of Thrust Performance on Position Relationship between RF Antenna and Magnetic Cusp of RF Plasma Thruster

IEPC-2017-344

Presented at the 35th International Electric Propulsion Conference
Georgia Institute of Technology • Atlanta, Georgia • USA
October 8 – 12, 2017

Yuya Oshio[1], Tomohiro Shimada [1], Hiroyuki Nishida [1],
[1] Tokyo University of Agriculture and Technology, Japan

Abstract: Electrodeless Radio Frequency (RF) Plasma Thruster was researched to improve the lifetime issue of the electric propulsion. The influences of positional relation between the RF antenna and the magnetic cusp on the thrust performance of the RF plasma thruster with nonuniform magnetic field were investigated by measuring the thrust and the exhaust plasma. The RF antenna was located at six positions, which is downstream position of 0 to 50 mm from the magnetic cusp. The RF antenna position at 10 mm downstream from the magnetic cusp had largest thrust performance (5.9 mN of thrust, 504 sec of specific impulse, 1.5% of thrust efficiency). It was shown that the exhaust plasma amount is largest at this RF antenna position by the exhaust plasma measurement. From these results, the knowledge about the suitable RF antenna position of the RF plasma thruster with nonuniform magnetic field was obtained.

Nomenclature

A_e	=	Cross-sectional area of discharge chamber exit, m^2
B	=	Magnetic field, T
F_{diamag}	=	Thrust by electromagnetic force, N
$F_{thermal}$	=	Thrust by thermal pressure, N
F_{total}	=	Total thrust, N
g	=	Gravitational acceleration, m/s^2
I_{sp}	=	Specific impulse, s
k_B	=	Boltzman's constant, 1.38×10^{-23} JK^{-1}
L	=	Thruster length, m
$\dot{m}$	=	Mass flow rate, kg/s
m_n	=	Mass of Ar, kg
p	=	Pressure, Pa
P_{source}	=	Input RF power, W
r_s	=	Discharge chamber radius, m
T	=	Temperature, K
Δt	=	Operation time (500 ms), s
η_t	=	Thrust efficiency

I. Introduction

A high power electric propulsion was applied in some mission in recently and several countries are now studying its technology intensively.[1-3] However, the damage of the electrode by the plasma is important issue. For example,

the Hall thruster which is the most promising candidate for the high power electric propulsion is prevented the damage of the electrode by the parallel magnetic field to the electrode.[4-5] In contrast, the electrodeless thruster was proposed. The electrodeless thruster utilizes the electrodeless discharge and the electrodeless plasma acceleration. The electroless thruster is expected significant extension of the lifetime of the electric propulsion. The thrust characteristics and the plasma physics of the helicon plasma thruster using the helicon discharge were investigated.[6-8] In addition, the plasma acceleration physics around the magnetic nozzle was researched.[9-10] Regarding the thrust performance, the simple helicon thruster including the Radio Frequency (RF) discharge and the magnetic nozzle achieved 8.1% of the thrust efficiency, which is ratio between the electric power and the thrust.[11] The research of the additional acceleration to improve the performance was conducted,[12-14] but the significant improvement has not been achieved yet. VASIMR achieved 72% of the thrust efficiency by additional Ion Cyclotron Resonance (ICR) heating,[15] although the required power of 200 kW is too high to use in the space in the near future. We aim to improve the thrust performance of the electrodeless RF plasma thruster in the low power condition. The typical RF plasma thruster with solenoid magnetic field is shown in Fig.1 (A). The propellant gas is ionized by RF discharge and the plasma is accelerated by the magnetic nozzle. In previous study, it was reported that the RF plasma thruster with nonuniform magnetic field including the magnetic cusp as shown in Fig.1 (B) can be improved the thrust efficiency.[16] However, at the thruster with nonuniform magnetic field, the thrust performance strongly depended on the RF antenna position and the magnetic field structure.[17] We revealed that the suitable RF antenna position is the downstream position from the magnetic cusp in previous study.[17] In order to optimize the RF plasma thruster, the investigation of the detailed RF antenna position effect on the thrust performance is necessity. The objective of this paper is to reveal the effect of the distance between the RF antenna and the magnetic cusp. In this paper, the RF antenna is located at downstream position of 0 mm to 50 mm than the magnetic cusp, and the thrust and the exhaust plasma flow are measured to investigate the RF antenna position effect on the thrust performance.

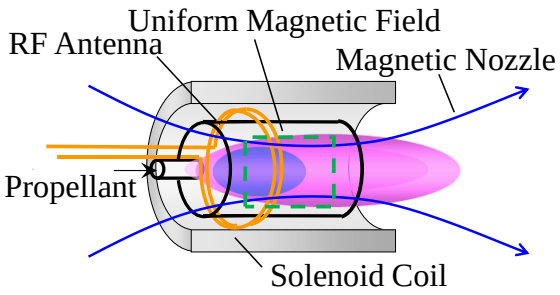

(A) Solenoid Type.

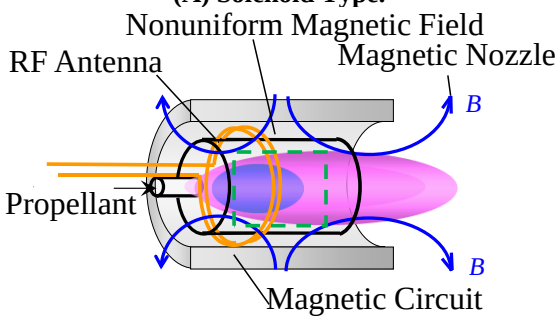

(B) Magnetic Cusp Type.

Figure 1. RF plasma thruster.

II. Experimental Setup and Conditions

A. RF Plasma Thruster with Magnetic Cusp

The schematic drawing of the RF plasma thruster is shown in Fig.1. The RF plasma thruster consists of the propellant gas system, the RF antenna for the RF discharge, the magnetic circuit for generating the magnetic field and the discharge chamber. A Pyrex tube of inner diameter of 23 mm and length 100 mm is employed as the discharge chamber. The triple loop coil of 38 mm of the diameter by ϕ2 mm copper wire is used as the RF antenna. The magnetic circuit consists of the bar type neodymium magnets placed at a circumferential position and the cylindrical type yoke. In order to evaluate the thrust characteristics in the moderate-size experimental set-up, a small-scaled model of the thruster is used in this study. The thrust by the magnetic nozzle is indicated by following equations[18]

$$F_{thermal} = 2\pi \int_0^{r_s} r p_e(r, z_0) dr \tag{1}$$

$$F_{diamag} = -2\pi \int_0^L \int_0^{r_p} \frac{B_r(r,z)}{B_z} \frac{\partial p_{e\perp}(r)}{\partial r} dr dz \tag{2}$$

$$F_{total} = F_{thermal} + F_{diamag} \tag{3}$$

where F_{thermal} is thrust by the pressure, F_{diamag} is the thrust by the electromagnetic force. In this paper, the total thrust as shown equation (3) is measured using the thrust stand. The thrust of the RF plasma thruster depends on the thruster size, but the RF discharge depends on the gas pressure, the magnetic field strength, RF power and so on. If the similar

figure thruster with the same gas pressure and suitable RF power to generate same plasma parameter is made, the thrust characteristics of small-scaled model thruster can be applied to full-scaled thruster.

B. Experimental Apparatus

Figure 2 shows the experimental apparatus. The experimental system consists of the RF plasma thruster head mount on the thrust stand, RF system, gas supply system, vacuum system and the measurement system. The thruster and measurement system are installed in the vacuum chamber (700 mm in diameter and 1200 mm long) with a pumping speed of 3000 L/s (N_2 equivalent) produced by a diffusion pump/rotary pumping system. The vacuum systems are pumped down to less than 10^{-3} Pa range without gas flow. The mass flow rate of the argon propellant gas is controlled by the mass flow controller and the propellant gas flows to the back plate of the thruster from the Ar gas tank. The RF system consists of the RF power supply (1000 W max and 13.56 MHz) and matching resistance. The RF discharge timing and the duration are controlled by the function generator. The RF plasma thruster is operated during 500 ms in this experiment.

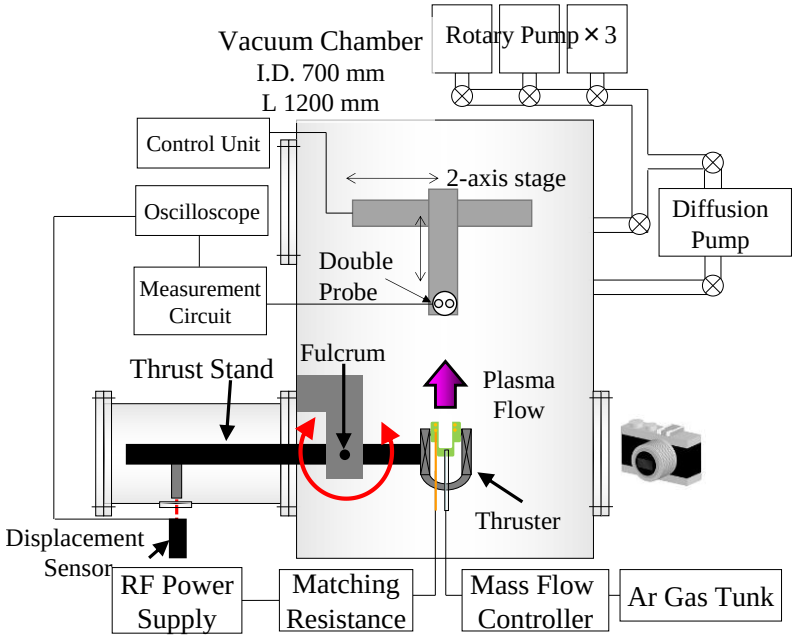

Figure 2. Experimental Setup.

C. Thrust Stand and Measurement Method

A torsion pendulum type thrust stand is employed for the thrust measurement. The thrust stand consists of left arm of 470 mm, right arm of 200 mm, laser displacement sensor to measure the displacement, and target for reflection of the laser and a coil-magnet actuator for the calibration as shown in Fig.3. The thrust stand receives the reaction force of the thrust and rotates around a rotary axis. The natural period of the pendulum is approximately 5.0 s, much longer than the MPS discharge duration of 0.5 ms. The impulse due to thrust acting on the pendulum stand can thus be considered to be of infinitely small duration. The impulse is measured by the first peak of the fitting curve. The response of the thrust stand to applied impulses is calibrated with impulses of known magnitude by coil-magnet actuator. The thrust is obtained by the operation time, Δt, as follows,

$$F = \frac{(F\Delta t)}{\Delta t} \tag{4}$$

The error bar of the thrust measurement is estimated by taking into account possible contributions from instrumental errors (dispersion of shot to shot, calibration errors) and curve fitting error.

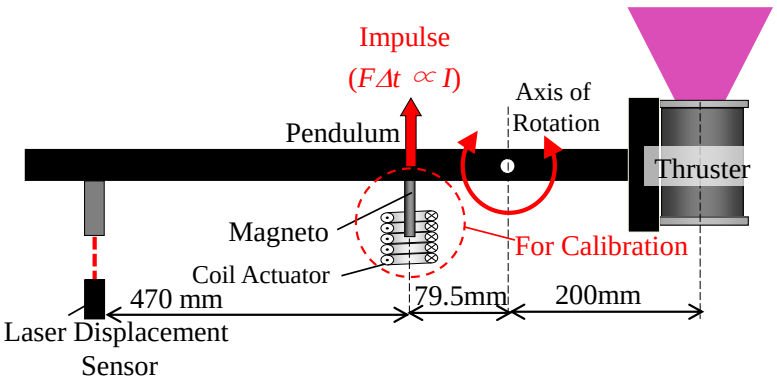

Figure 3. Torsion Pendulum Type Thrust Stand.

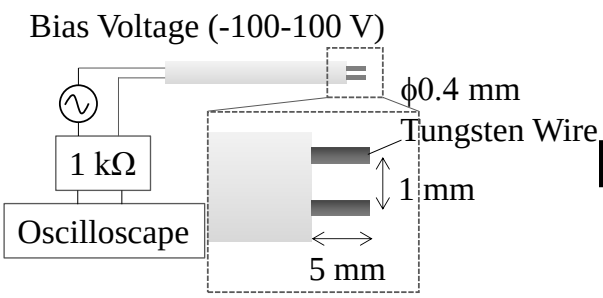

Figure 4. Schematic Diagram of Double Probe.

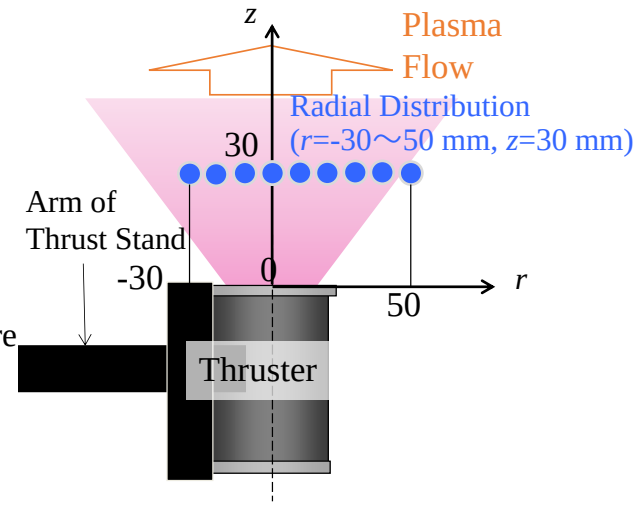

Figure 5. Measurement Positions of Exhaust Plasma.

D. Exhaust plasma measurement method

The double probe is used for the exhaust plasma measurement. The double probe consists of two tungsten wires, each 0.4 mm in diameter and 2.5 mm in length, housed in a mullite ceramics tube, as shown in Fig.4. The probe current is measured using by the voltage measured between both sides of 1 kΩ resistor. The electron number density is calculated by following equation using the current-voltage (I-V) characteristics by sweeping bias voltage.

$$I_{is} = \kappa n_e e S \sqrt{\frac{k_B T_e}{m_i}} \tag{5}$$

where I_{is} is ion saturation current, S is surface area of the probe electrode, T_e is the electron temperature decided by I-V curve[19] and n_e is the electron number density. To measure the radial distribution of the exhaust plasma, the plasma parameter is measured at the points shown in Fig.5 (with z and r axis as defined in Fig.5: The origin is the discharge chamber exit and the thruster center.).

E. Experimental Conditions and Evaluation Parameters

We investigate the thrust characteristics and the exhaust plasma characteristics for 1.2 mg/s of the mass flow rate and 100-1000 W of the RF power. We conducted the experiment at six RF antenna positions to investigate the RF antenna position effect on the thrust performance. The RF antenna positions and relation with the magnetic field are described in Fig.6. Figure 6 is calculated by the FEM software and the magnetic field line density of Fig.6 is adjusted to clearly understand the magnetic structure. The axial distribution of the magnetic field strength at the thruster center is shown in Fig.7. The maximum magnetic field is 54 mT at z=-20 mm. The magnetic cusp is located at z=-55 mm. The RF antenna is located at the downstream position than the magnetic cusp, because the downstream position than

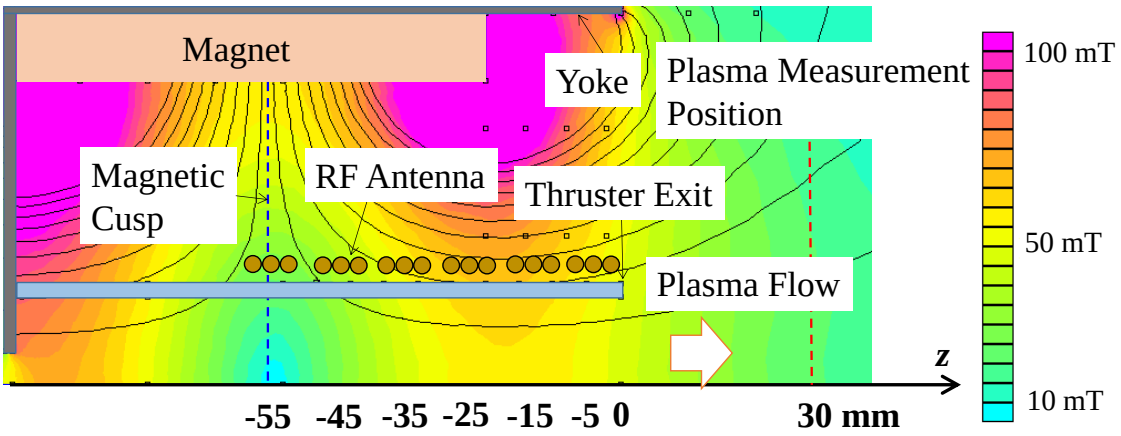

Figure 6. RF Antenna Positions and Magnetic Field Contour Figure.

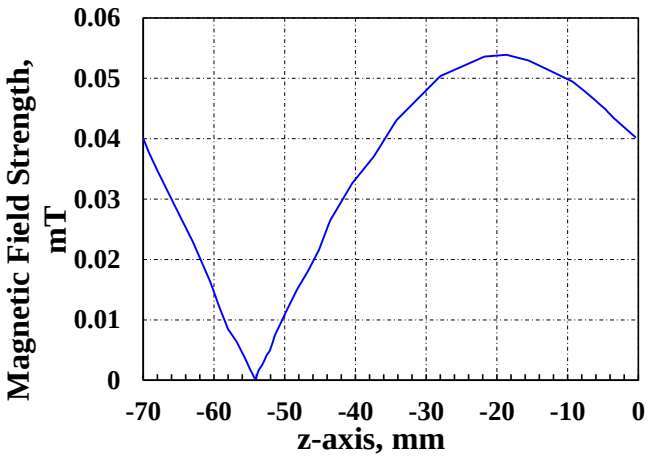

Figure 7. Magnetic Field Strength Distribution along Center Axis of Thruster.

Table 1 Experimental Conditions.

Propellant Gas	**Ar**
Mass Flow Rate	**1.2 mg/s**
Back Pressure	**~ 1.6×10^{-1} Pa**
Input Power	**100-1000 W**
Frequency	**13.56 MHz**
Operation Time	**500 ms**
RF Antenna Position	**z=-55, -45, -35, -25, -15, -5 mm**

the magnetic cusp is suitable as the RF antenna position in previous study. The RF antenna is located at z=-55 to -5 mm. The experimental conditions are listed in Table 1.

The thrust performance evaluation is performed following definitions, specific impulse I_{sp}, and thrust efficiency η_t. :

$$I_{sp} = \frac{F_{total}}{g\dot{m}_{eff}} \tag{6}$$

$$\eta_t = \frac{F_{total}^2}{2\dot{m}_{eff} P_{source}} \tag{7}$$

$$\dot{m}_{eff} = \dot{m} + \dot{m}_{ing} = \dot{m} + \frac{1}{4} A_e P_c \sqrt{\frac{m_n}{k_B T_n}} \tag{8}$$

where g, m_n, k_B, P_c and A_e are gravitational acceleration, mass of neutral particle, Boltzmann's constant, back pressure in the vacuum chamber and cross-sectional area at the discharge chamber exit, respectively. In this calculation, the temperature of neutral particle is assumed as the room temperature (300 k). The mass flow rate is estimated as the total of the inflow gas from upstream and the diffusive inflow from the downstream as shown in equation (8).

III. Experimental Results

A. Thrust Measurement Results

Figure 8 shows the thrust characteristics of the experimental condition of 1000 W and 1.2 mg in each RF antenna positions. The origin (z=0 mm) shows the discharge chamber exit and z=-55 mm is the magnetic cusp position. At the magnetic cusp positon, the thrust is smaller than it at z=-45 mm and z=-35 mm. The maximum thrust of 5.9 mN is obtained at z=0 mm. The thrust is decreased in further downstream than z=-45 mm. At z=-5 mm, the thrust is not almost generated. The thrust efficiency and specific impulse calculated by equation (6) and (7) are shown in Fig.9.

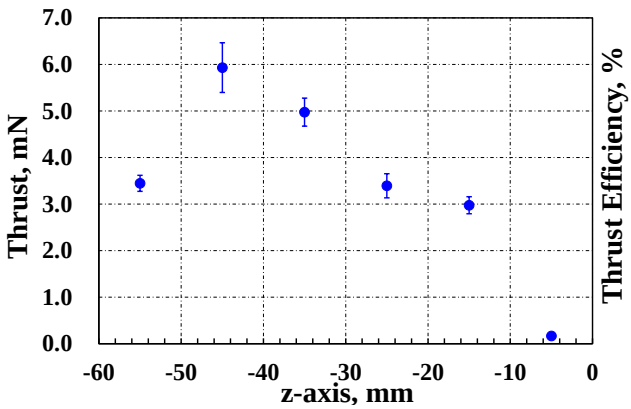

Figure 8. Thrust vs RF Antenna Position.

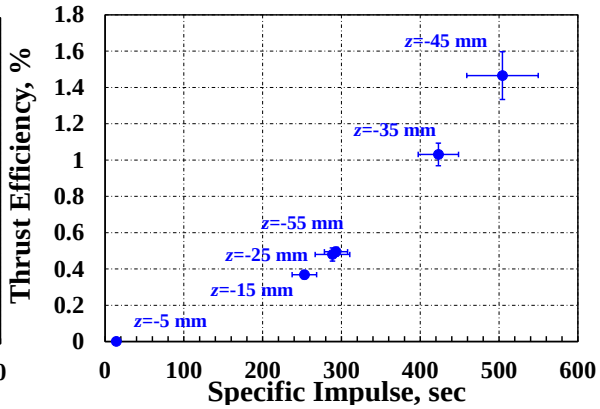

Figure 9 Thrust Efficiency vs Specific Impulse.

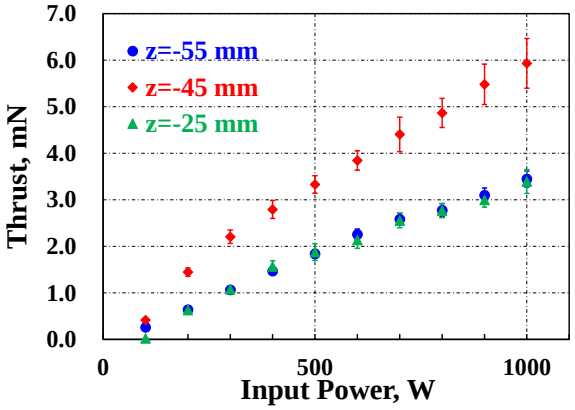

Figure 10. Thrust vs Input Power.

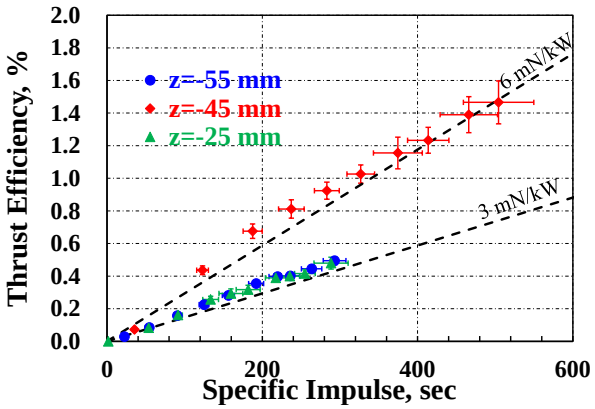

Figure 11 Thrust Efficiency vs Specific Impulse in each Input Power.

The maximum thrust performance in this experiment is 1.46% of the thrust efficiency and 504 sec of the specific impulse.

In order to investigate the input power dependencies on the thrust characteristics, the thrust versus input power measured ranging from 100 to 1000 W and results of 3 antenna positions are separately plotted in Fig. 10. At all antenna positions, the thrust increases with the input power increasing. The thrust at z=-45 mm is the largest thrust independently of input power. The thrust efficiency in three antenna positions is plotted as a function of the specific impulse in Fig.11. The RF antenna position of z=-45 mm provides the highest thrust performance. The performance at z=-45 mm is twice larger than the others. The dashed lines in Fig. 11 show the thrust-power ratio, which is the ratio of the thrust to the input power. The thrust-power ratio at z=-45 mm achieves the 6 mN/kW. From these results, it is shown that the suitable RF antenna position exists in the RF plasma thruster with nonuniform magnetic field including the magnetic cusp. The suitable RF antenna position in this operation conditions is downstream position of 10 mm than the magnetic cusp.

B. Exhaust Plasma Measurement Results

In order to investigate the reason of the suitable RF antenna position, the exhaust plasma structure is measured using by the double probe. We measure the radial distribution of the electron temperature and the electron number density at the downstream position of 30 mm from the discharge chamber exit (z=30 mm). The electron temperature is almost flat in the exhaust plasma at z=30 mm. The radial distribution of the electron number density at three RF antenna positions is shown in Fig.12. At z=-55 mm, the plasma is concentrated to the center of the exhaust plasma flow. However, there are two peaks of the electron number density at z=45 mm. This means that the exhaust plasma is formed doughnuts shape, which has small center plasma density. On the other hand, the exhaust plasma has broad structure at z=25 mm than other RF antenna positons. In order to measure the plasma flow structure, the electron number density at r=-40 mm is measured at only z=-25 mm. The two peak structure is obtained also at z=25 mm, although the peak is low. The one peak exists at r=-35 mm and the electron number density at peripheral part is larger than it at z=-55 mm. Therefore, it is shown that the exhaust plasma at z=-25 mm is broader than measurement range.

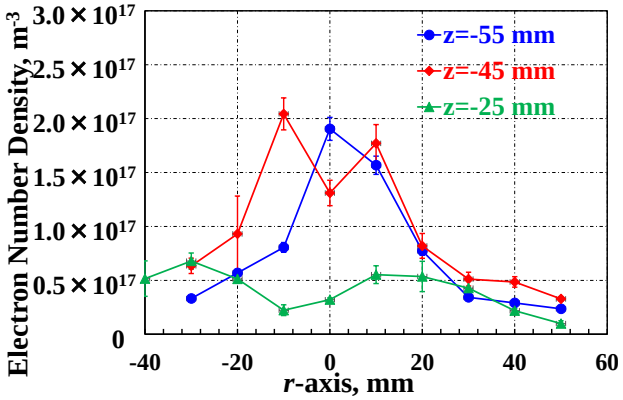

Figure 12. Radial Distribution of Electron Number Density.

IV. Discussion

The reason of the suitable RF antenna position is discussed in this section. The exhaust plasma amount is important parameter of the thrust. The largest exhaust plasma amount is obtained at *z*=45 mm as shown in Fig.12, because the peak number density is the highest and this condition generates the broadest high density plasma flow. On the other hand, the thrust at *z*=-55 mm and *z*=-25 mm is almost same, although the peak number density at z=-25 mm is smaller than it at z=-55 mm. This is because the exhaust plasma at z=-25 mm has broader plasma flow than it at z=-55 mm. We believe that the exhaust plasma amount at z=-55 mm and z=-25 mm is almost same. Therefore, the thrust characteristics depending on the RF antenna is corresponded to the exhaust plasma amount.

The RF discharge has suitable magnetic field strength, although the estimation of this is difficult by the combination of the several factor.[20] The each RF antenna position in this study is located at different magnetic field strength region as shown in Fig.7. The maximum thrust is obtained at low magnetic field region. In contrast, the thrust at the high magnetic field region is low. We consider that the suitable magnetic field strength in this RF antenna exists near the magnetic cusp. In addition, the peak of the electron number density transfers to peripheral part with moving the RF antenna to downstream than the magnetic cusp as shown in Fig. 11. The notional plasma flow structure in the discharge chamber is shown in Fig.13. This means that the plasma generation region approaches to near the RF antenna and the plasma diffusion across the magnetic field line is prevented. The wall loss is decreased by concentrating to the center of the discharge chamber, but the plasma is lost to the wall at the magnetic cusp position. From these factor of the RF antenna position effect (suitable magnetic field and wall loss), the thrust characteristics in each RF antenna is determined.

V. Conclusion

The effect of the RF antenna position on the thrust performance of the RF plasma thruster with nonuniform magnetic field including the magnetic cusp was investigated. The thrust characteristics and the radial distribution of the exhaust plasma were measured at six RF antenna positions, which are downstream position of 0 mm to 50 mm from the magnetic cusp. From these experiment, the following results are clarified.

・The RF antenna position at downstream position of 10 mm from the magnetic cusp has the largest thrust performance. The thrust that the RF antenna is located at the magnetic cusp position and further downstream position than 10 mm are decreased.

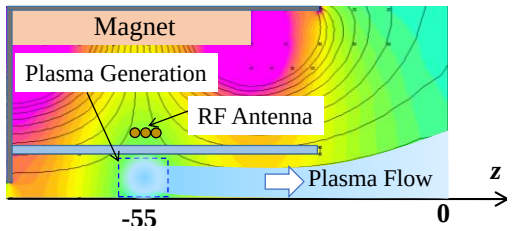

(A) RF Antenna Position: *z*=-55 mm.

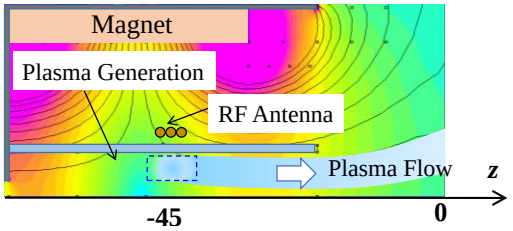

(B) RF Antenna Position: *z*=-45 mm.

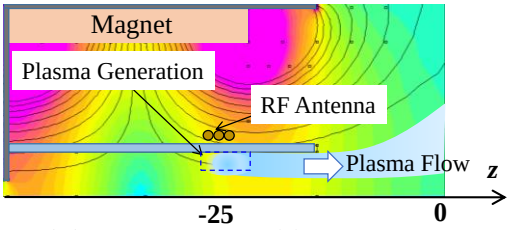

(C) RF Antenna Position: z=-25 mm.

Figure 13. Notional Plasma Flow Structures in Discharge Chamber.

・It is shown that the exhaust plasma amount is the largest at the maximum thrust condition by the exhaust plasma measurement. This is because the plasma generation efficiency is enhanced by the suitable magnetic field strength and the wall loss was decreased by the pinched plasma structure.

・It is shown that the thrust performance can be improved by locating the RF antenna at downstream position than the magnetic cusp and low magnetic field strength in low input power condition.

Acknowledgments

This research has been supported by a Grant-in-Aid for Young Scientists (B) (17K14874) from the Japan Society for Promotion of Science.

References

[1]Manzella, D. H., and Hack, K., "High-power solar electric propulsion for future NASA missions," 50th *AIAA/ASME/SAE/ASEE Joint Propulsion Conference*, Cleveland, AIAA 2014-3718, 2014.

[2]Matthias, G., Eric B., Guillaume, G., Nicoletta, W., Javier, P., Paolo, G., Waldemar, D., Andreas, F., Ulrich, S., and Giovanni, T., "Electric Propulsion Electronics Activities in Europe 2016," *52nd AIAA/ASME/SAE/ASEE Joint Propulsion Conference,* Salt Lake City, AIAA 2016-5032, 2016.

[3]Saito, Y., Kinefuchi, K., Nagao, N., Okita, K., and Kuninaka, H., "R&D Activities of Electric Propulsion in Japan." *In Proceedings of the 34th International Electric Propulsion Conference*, Kobe, IEPC-2015-28, 2015.

[4]Mikellides, I. G., Katz, I., Hofer, R. R., and Goebel, D. M., "Magnetic shielding of a laboratory Hall thruster. I. Theory and validation," *Journal of Applied Physics*, No,115, issue.4, 043303, 2014.

[5] Hofer, R. R., Goebel, D. M., Mikellides, I. G., and Katz, I.," Magnetic shielding of a laboratory Hall thruster. II. Experiments," *Journal of Applied Physics*, No,115, issue.4, 043304, 2014.

[6]Toki, K., Hashimoto, T., Makita, K., Shinohara, S., Hada, T., Ikeda, Y., & Funaki, I., "Small Helicon Source for Electrodeless Plasma Production and Electromagnetic Acceleration," *In 42nd AIAA/ASME/SAE/ASEE Joint Propulsion Conference & Exhibit* , Sacramento, AIAA-2006-4843, 2006.

[7] West. M.D., Charles. C., and Boswell, R.W., "Testing a Helicon Double Layer Thruster Immersed in a Space-Simulation Chamber", *Journal of Propulsion and Power*, Vol. 24, No. 1, pp. 134-141, 2008.

[8]Winglee, R., Ziemba, T., Giersch, L., Prager, J., Carscadden, J., and Roberson, B.R., "Simulation and laboratory validation of magnetic nozzle effects for the high power helicon thruster," *Physics of Plasmas*, Volume 14, Issue 6, 063501, 2007.

[9]Takahashi, K., Chiba, A., Komuro, A., & Ando, A. "Axial Momentum Lost to a Lateral Wall of a Helicon Plasma Source. " *Physical review letters*, Volume 114, Isuue 19, 195001, 2015.

[10]Ahedoa, E., and Merino, M.," Two-dimensional supersonic plasma acceleration in a magnetic nozzle" Physics of Plasmas, Volume 17, Issue 7, 073501, 2010.

[11]Takahashi, K., Charles, C., Boswell, R., and Ando, A.,"Performance improvement of a permanent magnet helicon plasma thruster," *Journal of Physics D: Applied Physics*, Volyme 46, Issue 35, 352001, 2013.

[12]Shinohara, S., Nishida, H., Tanikawa, T., Hada, T., Funaki, I., and Shamrai, K. P., "Development of electrodeless plasma thrusters with high-density helicon plasma sources," *IEEE Transactions on Plasma Science*, Volume 42, Issue 5, pp.1245-1254, 2014.

[13]Nishida, H., Nakamura, T., Shinohara, S., Matsuoka, T., Funaki, I., Tanikawa, T., and Shamrai, K. P., "Study on proof-of-principle of Lissajous acceleration for electrodeless helicon plasma thruster," *Frontier of Appl. Plasma Tech*, 5, pp.67-72, 2012.

[14]Carter, M., Ilin, A., Olsen, C. S., Squire, J. P., and Díaz, F. R. C., "Using VASIMR® for the Proposed Europa Mission," *AIAA SPACE 2014 Conference and Exposition*, AIAA 2014-4344, 2014.

[15]Squire, J.P. et al., "VASIMR® VX-200 Operation at 200kW and Plume Measurement, Future Plans and ISS EP Test Platform," *32nd International Electric Propulsion Conference*, Wiesbaden, IEPC-2011-154, 2011.

[16]Ito, S., Nakamura, T., Nishida, H., and Shinohara, S., "Performance of RF Plasma Thruster for Various Magnetic Field Configurations by Permanent Magnets," *Joint Conference of 30th International Symposium on Space Technology and Science*, Kobe, IEPC-2015-412 /ISTS-2015-b-412, 2015.

[17]Oshio, Y., Shimada, K., and Nishida, H., "Influence of Magnetic Cusp and Antenna Position on Thrust Performance of Electrodeless RF Plasma Thruster" The 57rd Conference on Aerospace Propulsion and Power, Naha, JSASS-2017-0062, 2017. (in Japanese)

[18]Takahashi, K., Charles C., and Boswell R. W., "Approaching the Theoretical Limit of Diamagnetic-Induced Momentum in a Rapidly Diverging Magnetic Nozzle," *Physical Review Letters*, Volume 10, 195003, 2013.

[19]Dote, T., "A New Method for Determination of Plasma Electron Temperature in the Floating Double Probe," *Japanese Journal of Applied Physics*, vol. 7, Number 8, pp. 964-965, 1968.

[20] Shamrai1, K.P., Shinohara, S., Virko, V.F., Slobodyan, V.M., Virko, V. Yu., and Kirichenko, G.S.,"Wave Stimulated Phenomena in Inductively Coupled Magnetized Plasmas", *Plasma Phys. Control. Fusion*, Vol. 47, pp. A307-A315, 2005.